MDPI

Article

Spatiotemporal Patterns of Ecosystem Restoration Activities and Their Effects on Changes in Terrestrial Gross Primary Production in Southwest China

Zhi Ding [1,2,3], **Hui Zheng** [3], **Ying Liu** [4], **Sidong Zeng** [4], **Pujia Yu** [1,2], **Wei Shi** [5] and **Xuguang Tang** [1,2,*]

1 Chongqing Jinfo Mountain Karst Ecosystem National Observation and Research Station, School of Geographical Sciences, Southwest University, Chongqing 400715, China; dingzhi11@mails.ucas.ac.cn (Z.D.); yupujia@swu.edu.cn (P.Y.)

2 State Cultivation Base of Eco-Agriculture for Southwest Mountainous Land, Southwest University, Chongqing 400715, China

3 Key Laboratory of Geospatial Technology for the Middle and Lower Yellow River Regions, Henan University, Kaifeng 475004, Henan, China; 10130103@vip.henu.edu.cn

4 Key Laboratory of Reservoir Aquatic Environment, Chongqing Institute of Green and Intelligent Technology, Chinese Academy of Sciences, Chongqing 400714, China; liuying311@mails.ucas.ac.cn (Y.L.); zengsidong@cigit.ac.cn (S.Z.)

5 State Key Laboratory of Resources and Environmental Information System, Institute of Geographic Sciences and Natural Resources Research, Chinese Academy of Sciences, Beijing 100101, China; shiw@lreis.ac.cn

* Correspondence: xgtang@swu.edu.cn

Abstract: Large-scale ecosystem restoration projects (ERPs) have been implemented since the beginning of the new millennium to restore vegetation and improve the ecosystem in Southwest China. However, quantifying the effects of specific restoration activities, such as afforestation and grass planting, on vegetation recovery is difficult due to their incommensurable spatiotemporal distribution. Long-term and successive ERP-driven land use/cover changes (LUCCs) were used to recognise the spatiotemporal patterns of major restoration activities, and a contribution index was defined to assess the effects of these activities on gross primary production (GPP) dynamics in Southwest China during the period of 2001–2015. The results were as follows. (1) Afforestation and grass planting were major restoration activities that accounted for more than 54% of all LUCCs in Southwest China. Approximately 96% of restoration activities involved afforestation, and these activities were mostly distributed around Yunnan Province. (2) The Breathing Earth System Simulator (BESS) GPP performed better than the Moderate Resolution Imaging Spectroradiometer (MODIS) GPP validated by field observation data. Nevertheless, their annual GPP trends were similar and increased by 12,581 g C m^{-2} d^{-1} and 13,406 g C m^{-2} d^{-1} for MODIS and BESS GPPs, respectively. (3) Although the afforestation and grass planting areas accounted for less than 1% of the total area of Southwest China, they contributed to more than 1% of the annual GPP increase in the entire study area. Afforestation directly contributed 14.94% (BESS GPP) or 24.64% (MODIS GPP) to the annual GPP increase. Meanwhile, grass planting directly contributed only 0.41% (BESS GPP) or 0.03% (MODIS GPP) to the annual GPP increase.

Keywords: ecological restoration; afforestation; LUCC; gross primary production; Southwest China

1. Introduction

Ecosystem restoration projects (ERPs) have been widely utilised across China to improve ecosystem conditions effectively [1–6]. Several ERPs, such as the Grain for Green Programme (GGP), Three-North Shelter Forest Programme, Karst Rocky Desertification Restoration Project (KRDRP), Natural Forest Protection Project and Returning Grazing Land to Grassland Project, have been implemented to counter land degradation, dust storms and soil erosion by re-establishing forest, shrub and/or grassland areas [4,7,8].

However, new plants in ERPs may be degraded and even die due to human disturbance and extreme climate events [9,10]. Overplanting trees may also aggravate water shortage due to excessive water consumption and reduce vegetation cover in arid and semiarid areas [11,12]. Monitoring spatiotemporal variations in restoration activities, such as afforestation and grass planting, and vegetation growth characteristics in areas with these activities can effectively help evaluate the effectiveness of ERPs and their ecosystems [13]. Although field studies can obtain accurate spatiotemporal distributions of these restoration activities, applying this method to large areas can be difficult due to extensive human resource and economic costs. Therefore, an effective method for determining the spatiotemporal distributions of afforestation and grass planting is necessary to assess the effectiveness of ERPs.

Remote sensing-based land use/cover change (LUCC) that directly reflects human-caused land use activities [14,15] is an effective method for exploring ERP-induced vegetation dynamics on a large scale [13,16,17]. Restoration activities, including afforestation and grass planting, which are largely linked to LUCC patterns converted from other land uses/covers into forests and grasslands, have been used to explore vegetation recovery [18]. For example, Zhao et al. [19] examined dominant systematic changes in land cover to recognise fundamental processes of land transition characteristics before and after the implementation of ecological programmes in the Loess Plateau in China. Qi et al. [13] developed an LUCC-based vegetation succession mapping method for evaluating the effects of restoration on karst vegetation in Southwest China. LUCC has also demonstrated that ecological restorations represent a major factor in increasing vegetation cover and greenness [8,17]. However, the increased occurrence of extreme climate events (e.g., drought and wildfire) due to climate change and the rapid expansion of human activities, such as agricultural reclamation, have exerted a considerable negative impact on vegetation recovery [9,10,20,21]. Therefore, the uncertain effects of ecological restorations on vegetation recovery should be investigated further.

Gross primary production (GPP), which is the total amount of organic carbon fixed by vegetation in terrestrial ecosystems, can reflect the growth characteristics and health status of these ecosystems [22–24]. Monitoring long-term and large-scale terrestrial GPP has progressed considerably due to remote sensing-based technology. Satellite-based GPPs, such as the Vegetation Photosynthesis Model [25], Moderate Resolution Imaging Spectroradiometer (MODIS) [26,27] and Breathing Earth System Simulator (BESS) GPPs [28,29], are major data sources for exploring terrestrial carbon cycles worldwide. Many studies have also successfully used GPP to assess the effectiveness of ecosystem restoration on vegetation recovery [4,5,30–32]. However, the application of these satellite-based GPP products to different regions may demonstrate some biases in performance due to the structures of models and uncertainties in various input parameters [33]. An intercomparison of results from multiple GPP products, such as BESS and MODIS GPPs, can help explore regional GPP dynamics without field data validation. However, regional-scale intercomparison studies are lacking.

A large continuous karst area in Southwest China [30,34] has undergone severe vegetation degradation and rocky desertification due to intense human exploitation since the middle of the last century [30,35]. The rocky desertification rate of this area is approximately 25,000 km^2 yr^{-1}, which is equal to the sandy desertification rate in Northwest China [35]. The low water-holding capacity of karst is due to its thin soil layer and numerous connected fissures from the bedrock layer to below the rooting zone or groundwater [36]. Severe water shortage persists in karst areas even during high precipitation [37]. In addition, the increase in karst rocky desertification aggravates the water shortage in karst regions [30,38–40]. ERPs, such as GGP and KRDRP, have been implemented since 2000/2001 to counter land degradation and relieve poverty [39]. Existing studies have demonstrated that these projects have considerably enhanced vegetation cover and greenness in this region [13,18,40]. However, research on the effects of specific restoration activities, such as afforestation and grass planting, on vegetation recovery remains limited.

In this study, long-term and successive climate change initiative land cover (CCI-LC) data were used to extract the spatiotemporal patterns of restoration activities and evaluate their effectiveness on vegetation recovery, as indicated by BESS and MODIS GPPs. This study primarily aims to (1) explore the spatiotemporal patterns of ecological restorations, (2) determine the intercomparison performance of the application of BESS and MODIS GPPs and their spatiotemporal patterns and (3) quantify the effects of major restoration activities on GPP changes from 2001 to 2015 in Southwest China.

2. Materials and Methods

2.1. Study Area

The study area (21°07′N–34°24′N and 97°26′E–110°01′E) (Figure 1) located in Southwest China includes the provinces of Sichuan, Guizhou, Yunnan and Guangxi and the city of Chongqing. Southwest China is the country's primary continuous distributor of karst. The karst in Guizhou, Yunnan and Guangxi Provinces is approximately 3.12×10^5 km^2 in size and accounts for nearly a quarter of the total karst area in China [35]. Abundant precipitation occurs in the study area, which is a typical subtropical region, with an annual average precipitation exceeding 1000 mm. The annual mean temperature ranges from 14 °C to 24 °C [41]. Major vegetation types are agricultural land, mixed forest and grassland (Figure 1B). The study area has undergone severe deforestation and rocky desertification since 1958 due to anthropogenic disturbances, and the rocky desertification area has reached 1.295 km^2 in 2005 [37]. ERPs, such as KRDRP, have been implemented since 2000/2001 to prevent severe vegetation degradation [39].
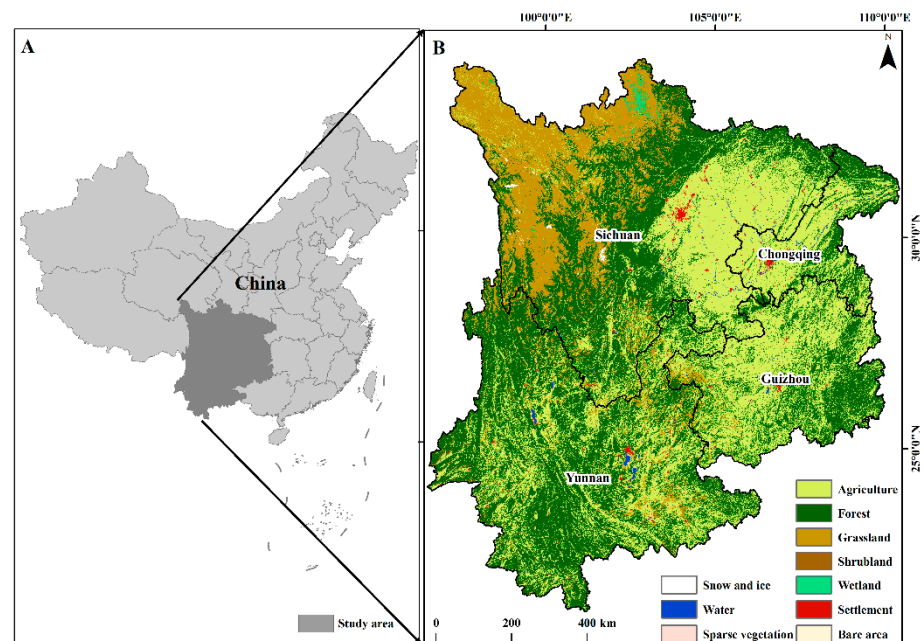

Figure 1. (**A**) Study area and (**B**) land CCI-LC in 2015.

2.2. Data Acquisition and Processing

Land cover data were downloaded from the website of the CCI-LC database (http://maps.elie.ucl.ac.be/CCI/viewer/download.php) (accessed on 29 January 2021), which is hosted by the European Space Agency. The data period is 2001–2015, and the spatial resolution of the data is 300 m. The land cover classification system (LCCS) has 22 classes for Level 1 and 31 classes for Level 2. The CCI-LC classification system was transferred to the commonly used Intergovernmental Panel on Climate Change land classification to extract data regarding restoration activities, and the results were compared with those from other land use data. CCI-LC was classified into 10 categories (Figure 1B). The overall

accuracy of LCCS Level 1 for CCI-LC is 75.38%, as validated by the GlobCover 2009 validation set. The accuracy of forest, agricultural land and grassland is 83%, 87% and 44%, respectively. Land use data were downloaded from the Data Centre of Resources and Environmental Sciences (RESDC, Chinese Academy of Sciences) (http://www.resdc.cn/) (accessed on 29 January 2021) [42,43] to validate their consistency from 2001 to 2015 and test the application of CCI-LC to the study area. RESDC land use data covered four periods (i.e., 2000, 2005, 2010 and 2015) with a spatial resolution of 1000 m and were interpreted from Landsat Thematic Mapper digital images and China–Brazil Earth Resource Satellite 1 data. The average interpretation accuracy for land use is approximately 92.9% in accordance with field surveys and random sample assessments [43]. Despite its high accuracy, the RESDC land use database cannot be used to extract annual land use changes because it covers only four periods. Changes from 2000 to 2015 for three primary land types, namely, agriculture, forest and grassland, were compared. Major land types in the two-source land data exhibited similar trends, i.e., a continuous decrease in agricultural lands, an increase in forests and a reduction in grasslands (Figure 2). The root-mean-square error (RMSE) of agricultural land reaches the maximum value probably due to the difference in land classification between RESDC and CCI-LC data [44]. The RMSE of forest and grassland is lower than that of agricultural land. Therefore, CCI-LC data were selected to investigate the trend of land use changes in the study area.
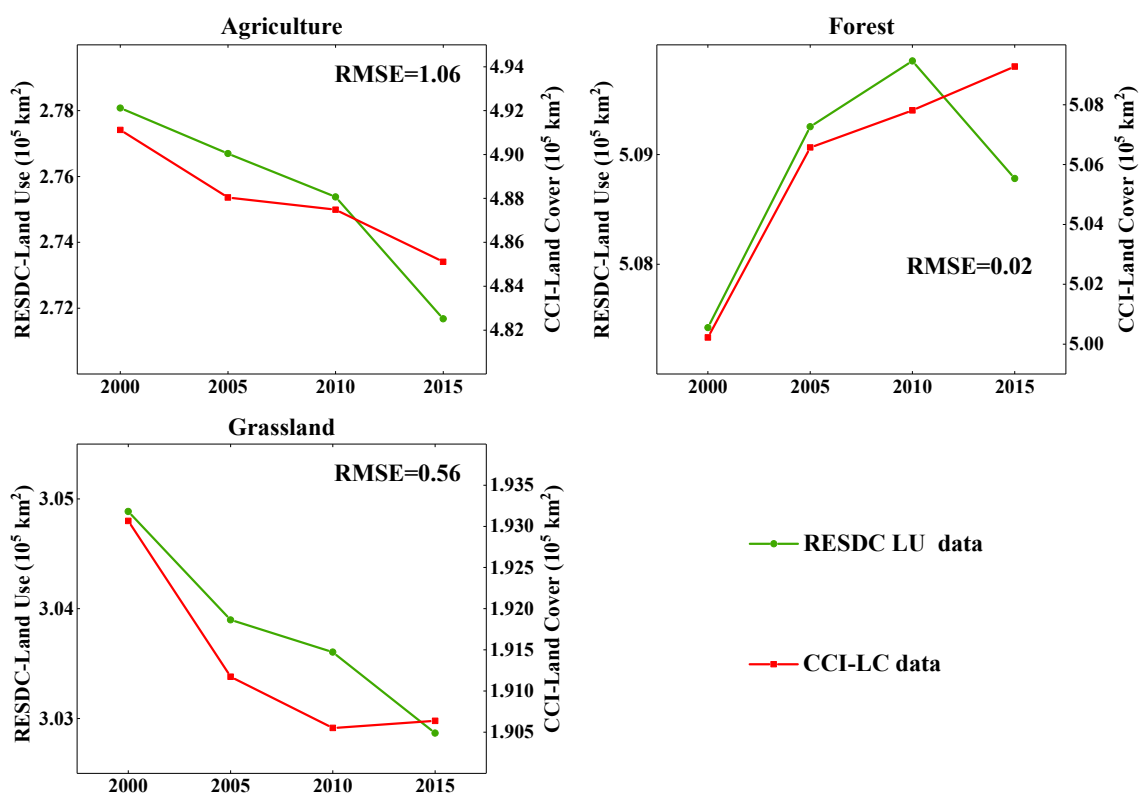
Figure 2. Consistency analysis of agricultural land, forest and grassland changes derived from the European Space Agency's CCI-LC and the RESDC of the Chinese Academy of Sciences in 2000–2015.

BESS and MODIS GPPs were used as the GPP source data to avoid the uncertainty of single-GPP source data. MODIS GPP, which is a version of the Numerical Terradynamic Simulation Group MOD17A3 (version 55) with a spatial resolution of 1 km, was downloaded from http://files.ntsg.umt.edu/data/NTSG_Products/MOD17/MOD17A3/ (accessed on 29 January 2021). Compared with its previous versions, MOD17A3 GPP (version 55) has been updated mostly due to the consideration of cloud effect and consistent meteorological forcing. It has been widely used in global carbon cycle analysis, ecosystem status assessment and environmental change monitoring. Additional information regard-

ing MODIS GPP data can be found in Zhao et al. [26,27]. BESS, a process-based model that generates GPP with high continuous spatiotemporal resolution, is comparable with in situ data and satellite-derived products (e.g., Max Planck Institute for Biogeochemistry) [28,29]. The new version of BESS products released in 2016 was downloaded from the website of the Environmental Ecology Lab (http://environment.snu.ac.kr/bess_flux/) (accessed on 29 January 2021). The spatial resolution of BESS GPP is also 1 km. Additional information regarding BESS GPP data can be found in Jiang and Ryu [28] and Ryu et al. [29]. In addition, the flux GPP data from the Xishuangbanna (2003–2010) site were collected to validate the performance of BESS and MODIS GPPs in the study area.

Annual precipitation and temperature data with a spatial resolution of 1 km in 2001–2015 were also downloaded from RESDC and produced by interpolating observations from 2472 meteorological stations in China.

2.3. Methods

Trajectory analysis that provides the spatiotemporal pattern of LUCC caused by natural and anthropogenic factors [45–47] can be utilised to recognise vegetation succession related to ERPs effectively [13]. Afforestation and grass planting have been adopted as major restoration activities to counter rocky desertification in Southwest China. Afforestation is generally defined as the replanting of trees in an area that was previously forested [48]. However, trees were also planted in previously unforested lands in the study area to improve ecological resistance in the karst region. To recognise the effects of natural and anthropogenic factors on vegetation cover in restoration areas, we used LUCC trajectory (LUCCT) to distinguish LUCCs driven by afforestation and grass planting (Table 1). Each cell in the interannual LUCCT to the overlaid annual land use and land cover data is analysed to recognise the spatiotemporal distribution of a restoration activity (Figure 3).

Table 1. Definition of LUCCT for afforestation and grass planting in Southwest China.

| Restoration Activity	LUCCT
Afforestation	Sparse vegetation → forest Agricultural land → forest Grassland → forest Shrubland → forest Bare area → forest
Grass planting	Sparse vegetation → grassland Agricultural land → forest Settlement → forest Bare area → forest

The actual GPP change in this study is divided into ERP-driven (e.g., afforestation and grass planting) and non-ERP-driven (e.g., self-growth and climate factors) GPP changes. An ERP-driven GPP change is defined as the difference between the GPPs of the previous year and the year of ERP implementation. A contribution index (CI) (Equation (1)), defined as the ratio of ERP-driven and actual GPP trends, was established to assess the contribution of ERP to GPP dynamics. The ERP-driven GPP trend represents the multiyear mean GPP change caused by afforestation or grass planting (Equation (2)). The actual GPP trend calculated using a linear regression model represents interannual GPP variations in afforestation and grass planting areas or the entire study area (Equation (3)). CI, ERP-driven GPP trend and actual GPP trend can be expressed as follows:

$$CI = \frac{|slope\_GPP_{ERP\text{-}driven}|}{|slope\_GPP_{actual} - slope\_GPP_{ERP\text{-}driven}| + |slope\_GPP_{ERP\text{-}driven}|} \times 100\% \quad (1)$$

$$slope\_GPP_{ERP\text{-}driven} = \frac{1}{n} \sum_{i=1}^{n} interGPP_i \quad (2)$$

$$slope\_GPP_{actual} = \frac{\sum_{i=1}^{n} GPP_i t_i - \frac{1}{n} \sum_{i=1}^{n} GPP_i \sum_{i=1}^{n} t_i}{\sum_{i=1}^{n} t_i^2 - \frac{1}{n} (\sum_{i=1}^{n} t_i)^2} \qquad (3)$$

where *CI* represents the percentage of GPP variations caused by afforestation and grass planting, $slope\_GPP_{ERP\text{-}driven}$ represents the multiyear mean GPP variations caused by afforestation and grass planting, $interGPP_i$ represents the interannual GPP variations between years $i-1$ and i, $slope\_GPP_{actual}$ represents the actual annual GPP trend from year i to year n in afforestation and grass planting areas, GPP_i represents GPP in year i and t_i represents year i.
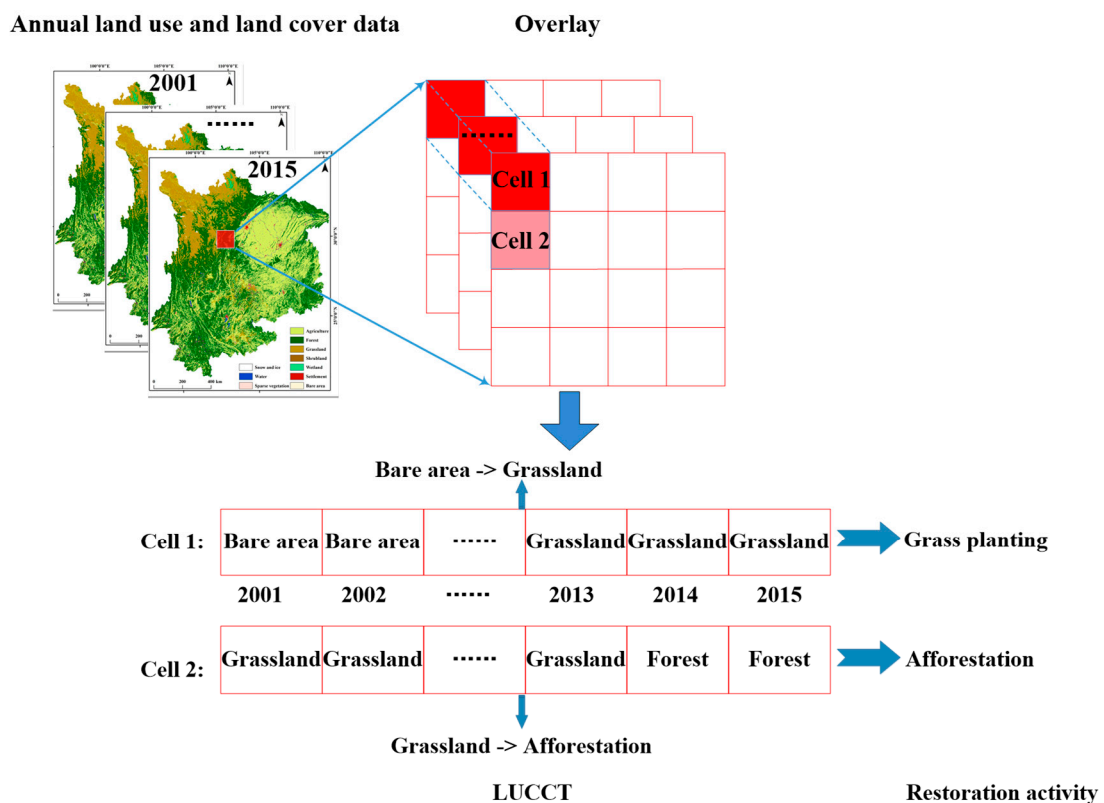
Figure 3. Grass planting and afforestation through LUCCT in 2000–2015.

Partial correlation based on Pearson's correlation was used to explore the effects of temperature or precipitation on GPP changes in each cell and avoid the interaction effects of the two variables. All analyses were conducted using MATLAB (The MathWorks Inc., Natick, MA, USA).

3. Results

### 3.1. Spatiotemporal Patterns of Ecological Restorations

The study area contained 10 LUCCTs that represent 98% of all LUCCs in 2001–2015 (Figure 4). The LUCCT based on its area percentage relative to all patterns demonstrated the following order: agricultural land → forest, shrubland → forest, agricultural land → settlement, forest → agricultural land, grassland → agricultural land, grassland → forest, forest → grassland, agricultural land → grassland, shrubland → agricultural land, grassland → settlement. Major restoration activities were afforestation (agricultural land → forest, shrubland → forest, grassland → forest), grass planting (agricultural land → grassland) and major land conversions that surpassed 54% of all LUCCs. To date, 51.66% and 2.34% of LUCC account for afforestation and grass planting, respectively. Therefore, afforestation, which accounted for 96% of major restorations, was the dominant restoration

type in the study area. Meanwhile, LUCCTs related to extreme climate events, such as drought, wildfire and human disturbance, including agricultural reclamation, were rare. This finding indicated that extreme climate events and human disturbance exerted minimal negative impact on vegetation recovery in restoration areas.

Figure 5 shows that the majority of afforestation is distributed around Yunnan Province. However, over 34% of the total afforestation area occurred in 2004 and was mostly distributed outside of Yunnan Province. The afforestation area exhibited a decreasing trend after 2004 but increased significantly in 2014. By comparison, grass planting mostly occurred around the northeastern area of Sichuan Province in the periods of 2007–2009 and 2000–2003. The area of grass planting presented an N-shaped variation, and peaks occurred in 2008 and 2012.
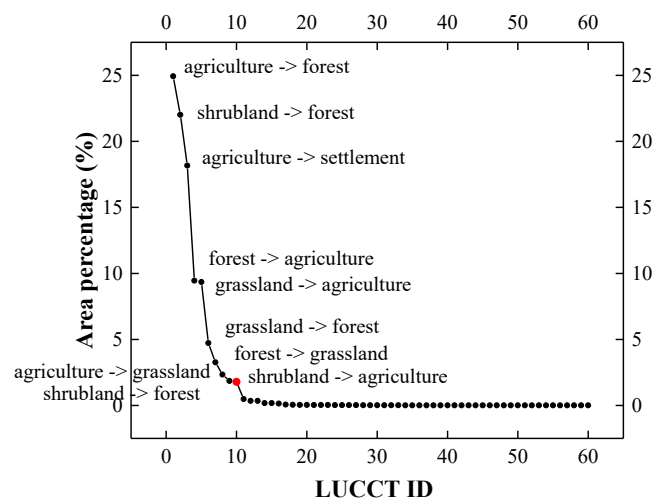

Figure 4. Area percentage of each LUCCT amongst all LUCCTs in descending order in 2001–2015. The red point represents the boundary of major and minor LUCCTs, and the LUCCT ID is defined by the percentage of area in descending order.
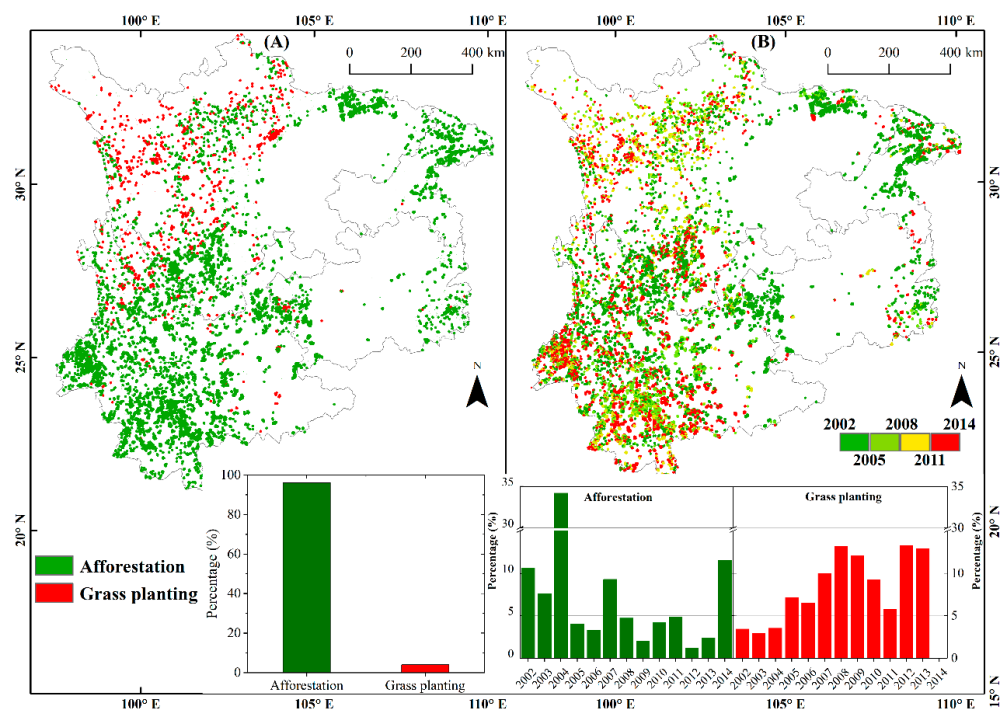
Figure 5. (**A**) Spatial distributions of annual afforestation and grass planting in 2002–2015 and (**B**) their implementation time.

3.2. Performance of the Application of MODIS and BESS GPPs in Southwest China

Compared with MODIS GPP, BESS GPP demonstrates higher consistency with flux observation GPP data (Figure 6A). The coefficient of determination (R^2) of seasonal BESS and flux GPPs from 2003 to 2010 reached 0.59 with an RMSE of 1.30 g C m^{-2} d^{-1}. The R^2 of MODIS and flux GPPs was only 0.01 with a high RMSE of 2.73 g C m^{-2} d^{-1}. The low R^2 value of MODIS and flux GPPs was largely due to the difference in their trends from March to September in one year (Figure 6B).
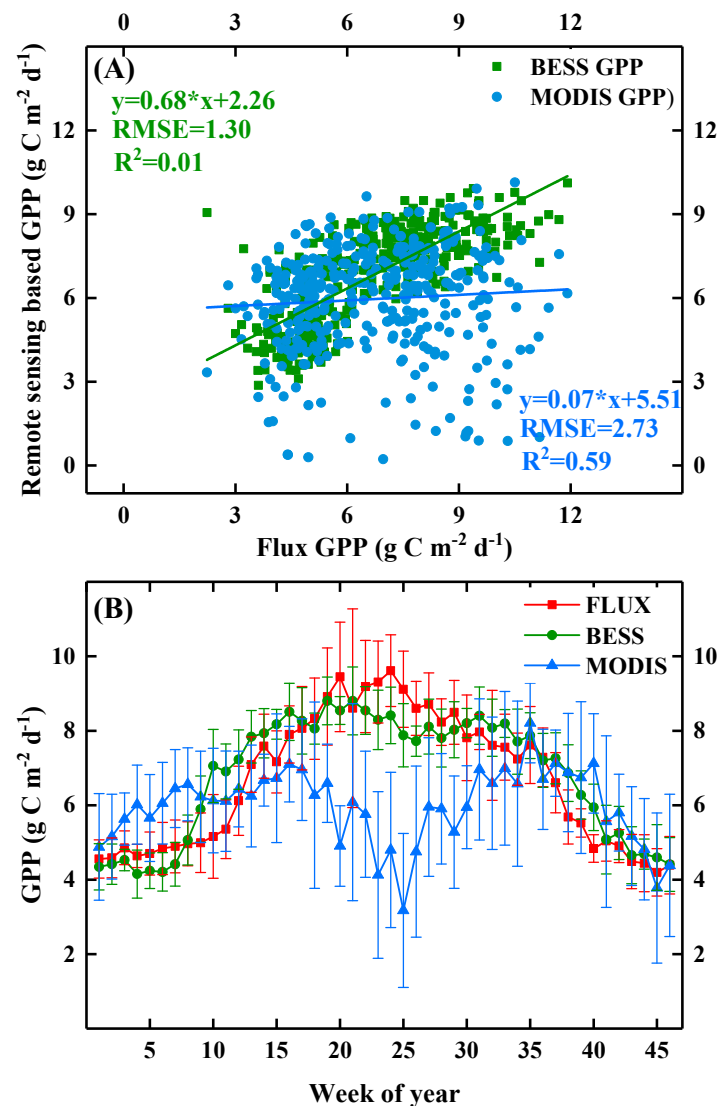

Figure 6. (**A**) Consistency analysis of MODIS GPP, BESS GPP and flux observations from Xishuangbanna and (**B**) comparison of their seasonal trends in 2003–2010.

MODIS and BESS GPPs presented an increasing trend in 2001–2015 (Figure 7A,B). Pixel counts with an increasing trend surpassed 72% and 76% of the total area in accordance with MODIS and BESS data, respectively. The trends of these pixels with a GPP increase were within the range of 0–0.15 g C m^{-2} d^{-1}, with most of the pixels distributed around the southeastern area of Yunnan, adjacent places of the three provinces and Chongqing City and the northwestern region of the study area. Overall, the sum of the entire GPP trend was 12,581 g C m^{-2} d^{-1} and 13,406 g C m^{-2} d^{-1} for MODIS and BESS GPPs, respectively. In addition, nearly 90% of the pixels with significant changes ($p < 0.05$) also exhibited an increasing trend (Figure 7C,D). The spatial distribution of pixels with significantly

increasing trend was similar for MODIS and BESS GPPs and largely distributed around the southeastern area of Yunnan and adjacent places of the three provinces and Chongqing City.
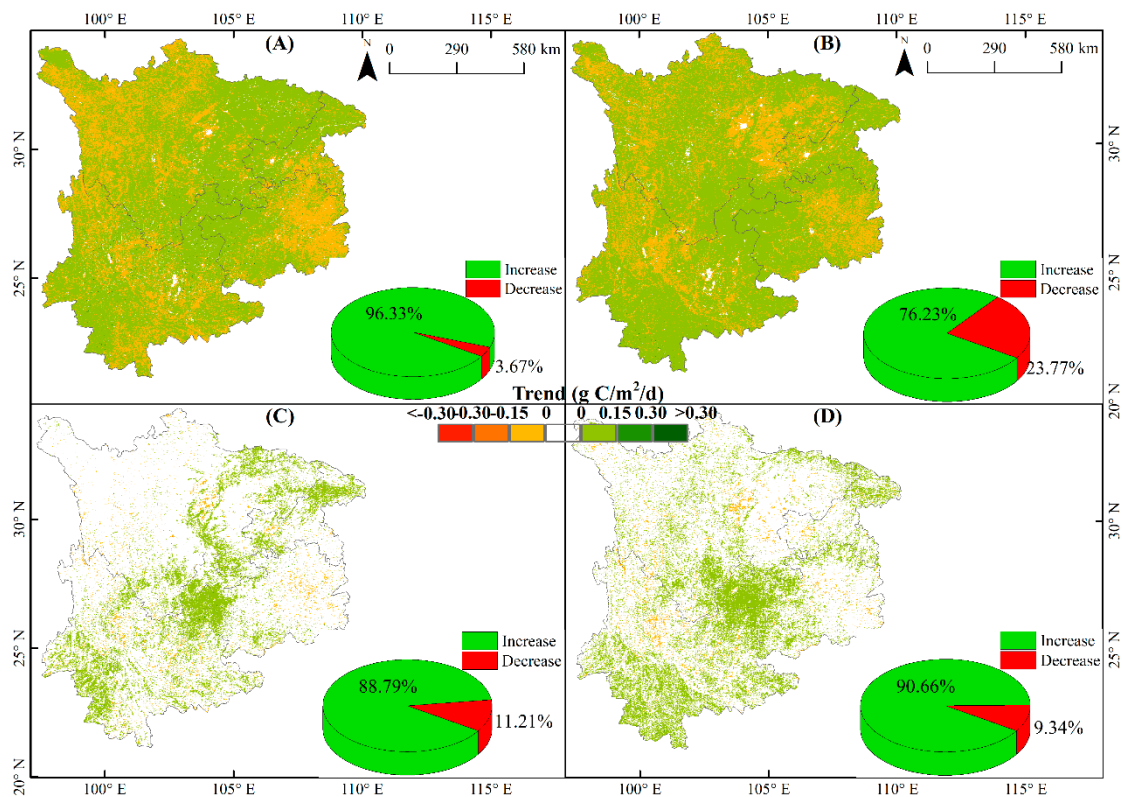
Figure 7. Complete and significant ($p < 0.05$) trends for (**A**,**C**) MODIS and (**B**,**D**) BESS GPPs.

3.3. Contribution of Major Restorations to the Increase in GPP

The actual annual GPP in afforestation and grass planting areas presented a significantly increasing trend (169.66 g C m^{-2} d^{-1} and 135.17 g C m^{-2} d^{-1} for BESS and MODIS GPPs, respectively). Nearly 14.97% (indicated by BESS GPP) or 25.04% (indicated by MODIS GPP) of the actual annual GPP increase was directly contributed by afforestation and grass planting. The majority of the contribution originating from afforestation accounted for nearly 14.94% (indicated by BESS GPP) or 24.64% (indicated by MODIS GPP) of the actual annual GPP increase (Figure 8). Grass planting caused a slight GPP increase (0.05 g C m^{-2} d^{-1} and 0.55 g C m^{-2} d^{-1} for BESS and MODIS GPPs, respectively) and contributed only 0.41% (indicated by BESS GPP) or 0.03% (indicated by MODIS GPP) of the actual annual GPP increase (Figure 8). However, grass planting contributed a considerable actual GPP increase (38% and 27% for BESS and MODIS GPPs, respectively) to the grass planting area (Table 2). Similar to the afforestation area, the maximum GPP increase caused by afforestation also occurred in 2004 and then demonstrated a decreasing trend after this year (Figure 9). However, the interannual GPP change caused by grass planting was different from that of the annual grass planting area (Figure S1). Afforestation and grass planting areas contributed a total of over 1.1% (MODIS GPP) or 1.2% (BESS GPP) to the annual GPP increase in Southwest China for the entire study area.
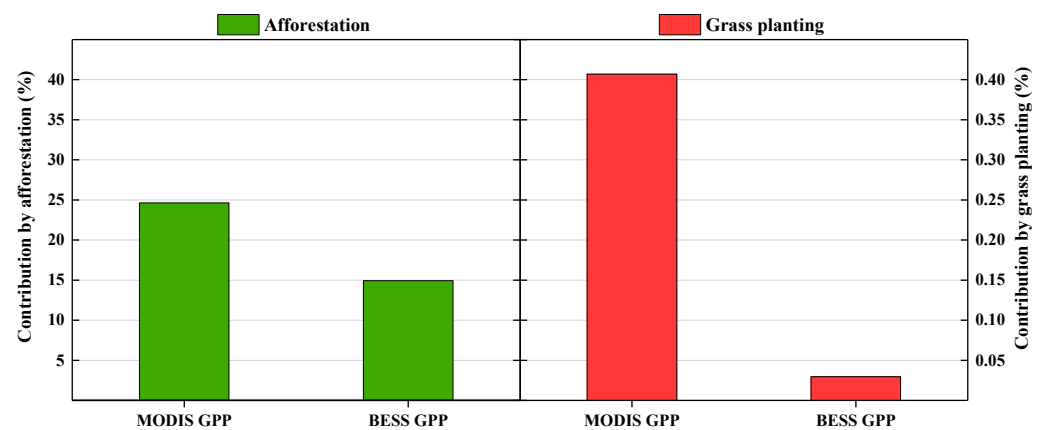
Figure 8. Contributions of afforestation and grass planting to the actual GPP increase in afforestation and grass planting areas during the period of 2001–2015.

Table 2. ERP-driven (afforestation and grass planting) and actual GPP trends from 2001 to 2015.

| Area	BESS GPP Trend (g C m^{-2} d^{-1})			MODIS GPP Trend (g C m^{-2} d^{-1})		
	ERP-Driven	Actual	CI (%)	ERP-Driven	Actual	CI (%)
Afforestation	25.35	169.69	14.94	33.30	136.11	24.47
Grass planting	0.05	−0.03	38.46	0.55	−0.94	26.96
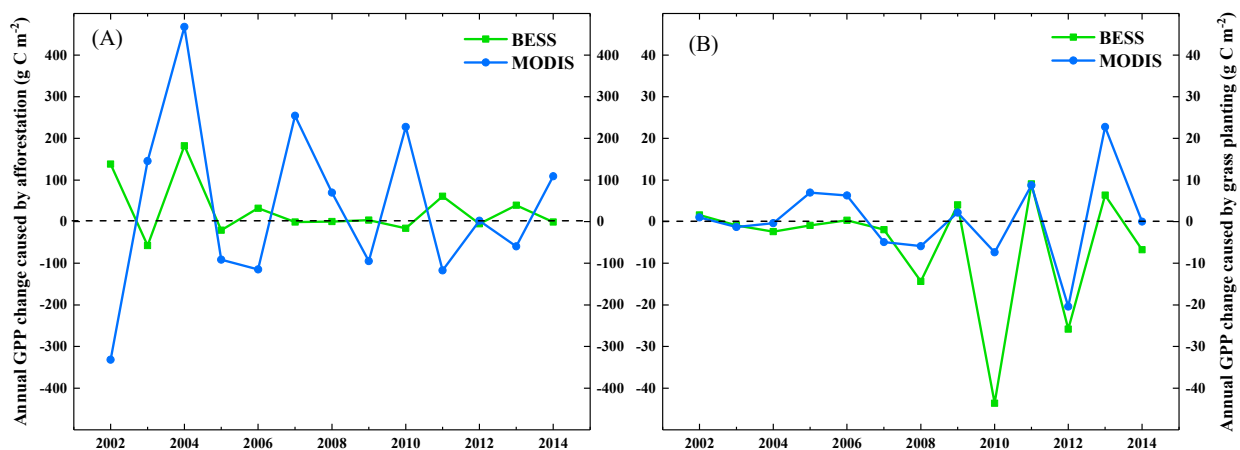
Figure 9. Annual GPP changes caused by (**A**) afforestation and (**B**) grass planting during the period of 2001–2015.

4. Discussion

4.1. Major Restoration Activities in 2001–2015

Similar to the findings of a previous study in Southwest China during the period of 2001–2015, our results showed that afforestation was the dominant land cover change [30]. The large area of afforestation was attributed to GGP and KRDRP. These ERPs were launched to re-establish forests, shrublands and grasslands and counter severe rocky desertification in Southwest China since 2000/2001 [18,39]. Forests have high economic value and easily survive in the study area with abundant precipitation and warm temperature. Therefore, planting trees was the preferred method for improving vegetation cover [18,49] and the forest area substantially increased during this period [18]. Our results also showed that more than 48% of the entire afforestation area was converted from agricultural land (Figure 10). Consistent with the results of previous studies, this finding indicated that ERPs were successfully implemented in the study area [50]. Existing studies also found that afforestation considerably relieved land degradation due to the large conversion of

desertification areas into forests [30,51]. Therefore, afforestation has become the dominant restoration activity that remarkably enhances vegetation cover in Southwest China.
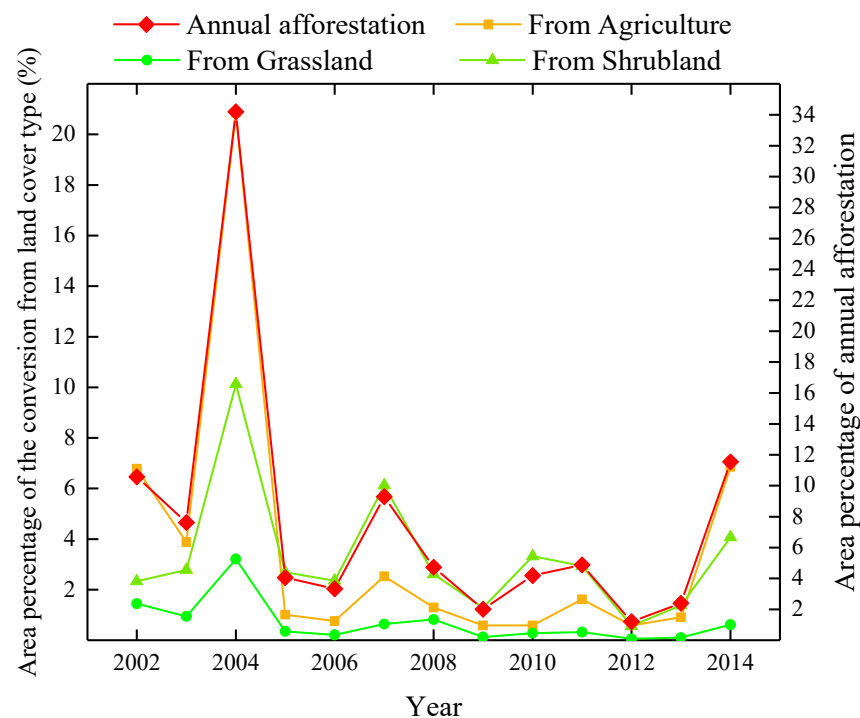
Figure 10. Original land cover types converted into forest and their area percentage in relation to the total afforestation area from 2001 to 2015.

4.2. Constrasting Performance of MODIS and BESS GPPs in Southwest China

Our results showed that seasonal BESS GPP demonstrated consistent seasonal trajectory with flux observation data and a low RMSE of approximately 1.30 g C m^{-2} d^{-1}. The single hump-shaped trend (Figure 6B) of seasonal BESS GPP is consistent with the growing trajectory of normal vegetation and similar to the results of previous studies [28,33]. By comparison, MODIS GPP exhibited an unusually lower value in growing seasons and higher value in other seasons (Figure 6B); this result was also reported in a previous study [33]. The possible reason for this finding was that the algorithms of the MODIS models disregarded the differences in C$_3$/C$_4$ plants [29]. Consequently, MODIS overestimated GPP during the periods from January to March and from October to December and underestimated GPP from March to September. In addition, BESS GPP also exhibited consistent interannual variability with flux data from 2000 to 2010 (Figure 11A). This finding is likely due to the improvement in the process-based model of BESS with an adequately modelled spring phenology and soil thawing that largely contributed to the consistent trajectory [28]. Both BESS and MODIS GPPs can spatially capture total interannual variations and presented increasing trends (Figure 7). However, the two GPP products failed to capture the large GPP decrease (Figure 11B) caused by an extreme drought during the period of 2009–2010 [52,53]. Overall, BESS GPP performed better than MODIS GPP and field observation data.
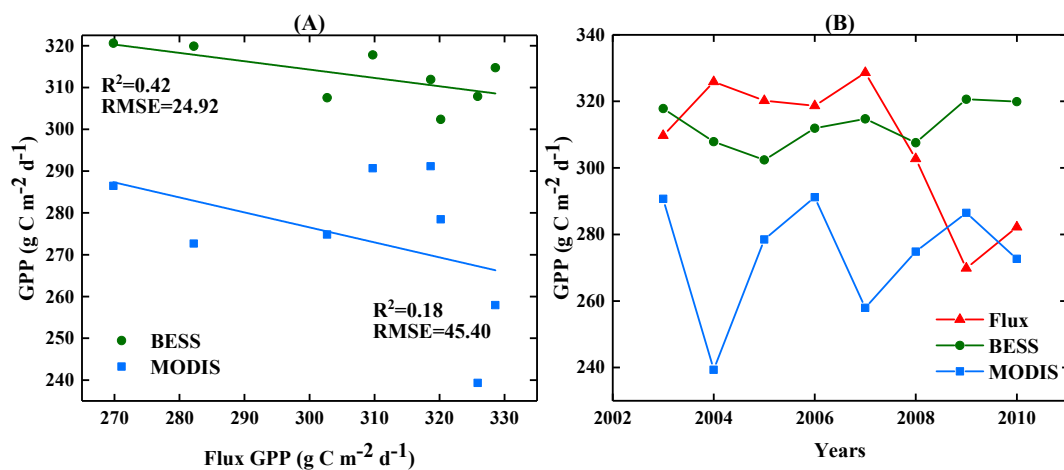
Figure 11. (**A**) Evaluation of BESS GPP and MODIS GPP products against flux observations from Xishuangbanna and (**B**) the annual variability of flux GPP, BESS GPP, and MODIS GPP during the period of 2003–2010.

4.3. Contribution of Major Restoration Activities to GPP Increase

Afforestation significantly contributed to GPP increase (14.9% and 24.6% for BESS and MODIS GPPs, respectively) in afforestation and grass planting areas due to its large area coverage. Over 54% of LUCC areas and 98% of major restoration areas were attributed to afforestation. In addition, planting trees can considerably improve vegetation cover and production due to the high biomass of trees. Although grass planting contributed to a small proportion of the total actual GPP (0.03% and 0.41% for BESS and MODIS GPPs, respectively) in the entire restoration area, it contributed over a quarter of the actual GPP increase in the grass planting area. In addition, grass planting was mostly distributed around the west of Sichuan and cannot be replaced by afforestation due to the environment of the fragile ecosystem, such as the occurrence of water deficit. Therefore, grass planting also plays an important role in vegetation recovery in the study area. Overall, the annual GPP increase in afforestation and grass planting areas exerted a positive effect on GPP increase in the entire study area. Afforestation and grass planting areas contributed more than 1% of the annual GPP increase because they accounted for less than 1% of the total study area. In addition, ERP also includes closed hillside afforestation to conserve forests and nature reserve areas [4], which are difficult to recognise in remote sensing images and disregarded in the current study. Therefore, the contribution of ERPs to GPP increase may be larger than that reported in this work.

Generally, precipitation and temperature have a large impact on the dynamics of vegetation growth such as the normalised difference vegetation index [54–56], leaf area index and GPP [57]. In this study, annual precipitation and temperature exerted a small influence on GPP dynamics in restoration areas. Only a minor part (i.e., 8% for BESS GPP and 17% for MODIS GPP) of GPP exhibited significant correlations ($p < 0.05$) with the annual precipitation and temperature in the entire restoration area (Figure 12). Furthermore, this influence due to precipitation and temperature might lead to a decrease in the GPP (Table 3). The GPP decrease was largely related to the reductions in annual precipitation and temperature, which were also found in a previous study conducted during the same period [58].

In terms of climate change, vegetation recovery through ERPs should be the focus of future investigations to alleviate the GPP decrease caused by precipitation and temperature. Even if an extreme drought occurred during the period of 2009–2010 [52,53], annual GPP in the afforestation area exhibited minimal decrease and even increased as shown by MODIS GPP (Figure 9). As an effective method for improving vegetation recovery, ERPs can help enhance an ecosystem by improving vegetation structure and weakening the negative effects of climate factors (e.g., precipitation and temperature) on GPP dynamics. In addition, trees and grasses resulting from afforestation and grass planting will grow as

time progresses and continuously contribute to the improvement of the regional ecosystem environment. Therefore, ERPs, including afforestation and grass planting, will increase GPP and reduce an ecosystem's sensitivity to climate perturbations.
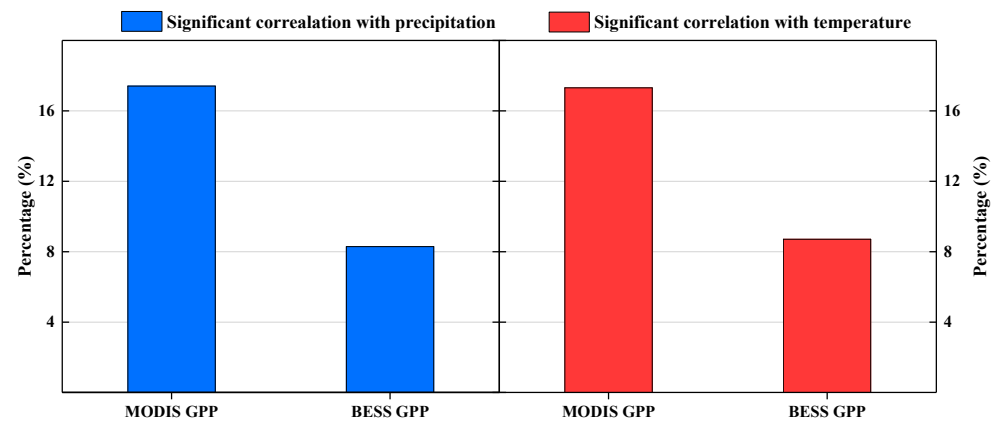
Figure 12. Area percentage of GPP significantly correlated ($p < 0.05$) to precipitation and temperature in restoration areas.

Table 3. Area percentages of increasing and decreasing GPPs significantly correlated ($p < 0.05$) to precipitation and temperature in restoration areas.

GPP Trend	Precipitation		Temperature	
	MODIS	**BESS**	**MODIS**	**BESS**
Increase	20.42	37.70	20.42	37.80
Decrease	79.58	62.30	79.58	62.20

5. Conclusions

Long-term and successive ERP-driven LUCCs were explored to determine the spatiotemporal distributions of major restoration activities and their effects on GPP dynamics in Southwest China during the period of 2001–2015. The following conclusions can be drawn from this study. (1) Afforestation and grass planting were the major restoration activities that accounted for more than 54% of all LUCCs in Southwest China. Afforestation accounted for approximately 96% of all restoration activities, and the remainder was related to grass planting. (2) BESS GPP performed better than MODIS GPP validated by field observation data. Nevertheless, their annual GPP trends were similar and increased by 12,581 g C m^{-2} d^{-1} and 13,406 g C m^{-2} d^{-1} for MODIS and BESS GPPs, respectively. (3) Afforestation and grass planting areas were less than 1% of the total area of Southwest China but contributed to more than 1% of the annual GPP increase in the entire study area. Moreover, 14.94% (BESS GPP) or 24.64% (MODIS GPP) of the annual GPP increase in afforestation and grass planting areas was directly contributed by afforestation and only 0.41% (BESS GPP) or 0.03% (MODIS GPP) of the annual GPP increase was directly contributed by grass planting. However, grass planting contributed a considerable actual GPP increase (38% and 27% for BESS and MODIS GPPs, respectively) in the grass planting area. Restoration activities, such as closed hillside afforestation, for the conservation of forests and nature reserve areas were disregarded in this study. Therefore, the actual contribution of ERPs to GPP increase may be larger than that reported in this work.

References

1. Tong, X.; Wang, K.; Yue, Y.; Brandt, M.; Liu, B.; Zhang, C.; Liao, C.; Fensholt, R. Quantifying the effectiveness of ecological restoration projects on long-term vegetation dynamics in the karst regions of southwest china. *Int. J. Appl. Earth Obs. Geoinf.* **2017**, *54*, 105–113. [CrossRef]
2. Tan, M.; Li, X. Does the green great wall effectively decrease dust storm intensity in china? A study based on noaa ndvi and weather station data. *Land Use Policy* **2015**, *43*, 42–47. [CrossRef]
3. Li, G.; Sun, S.; Han, J.; Yan, J.; Liu, W.; Wei, Y.; Lu, N.; Sun, Y. Impacts of chinese grain for green program and climate change on vegetation in the loess plateau during 1982–2015. *Sci. Total Environ.* **2019**, *660*, 177–187. [CrossRef] [PubMed]
4. Niu, Q.; Xiao, X.; Zhang, Y.; Qin, Y.; Dang, X.; Wang, J.; Zou, Z.; Doughty, R.B.; Brandt, M.; Tong, X. Ecological engineering projects increased vegetation cover, production and biomass in semi-arid and sub-humid northern china. *Land Degrad. Dev.* **2019**. [CrossRef]
5. Ma, H.; Lv, Y.; Li, H. Complexity of ecological restoration in china. *Ecol. Eng.* **2013**, *52*, 75–78. [CrossRef]
6. Wen, X.; Théau, J. Assessment of ecosystem services in restoration programs in china: A systematic review. *Ambio* **2020**, *49*, 584–592. [CrossRef]
7. Lu, F.; Hu, H.; Sun, W.; Zhu, J.; Liu, G.; Zhou, W.; Zhang, Q.; Shi, P.; Liu, X.; Wu, X. Effects of national ecological restoration projects on carbon sequestration in china from 2001 to 2010. *Proc. Natl. Acad. Sci. USA* **2018**, *115*, 4039–4044. [CrossRef]
8. Piao, S.; Yin, G.; Tan, J.; Cheng, L.; Huang, M.; Li, Y.; Liu, R.; Mao, J.; Myneni, R.B.; Peng, S. Detection and attribution of vegetation greening trend in china over the last 30 years. *Glob. Chang. Biol.* **2015**, *21*, 1601–1609. [CrossRef]
9. Wang, H.; Liu, G.; Li, Z.; Ye, X.; Fu, B.; Lv, Y. Impacts of drought and human activity on vegetation growth in the grain for green program region, china. *Chin. Geogr. Sci.* **2018**, *28*, 470–481. [CrossRef]
10. Zhao, A.; Zhang, A.; Liu, J.; Feng, L.; Zhao, Y. Assessing the effects of drought and "grain for green" program on vegetation dynamics in china's loess plateau from 2000 to 2014. *Catena* **2019**, *175*, 446–455. [CrossRef]
11. Cao, S. Impact of china's large-scale ecological restoration program on the environment and society in arid and semiarid areas of china: Achievements, problems, synthesis, and applications. *Crit. Rev. Environ. Sci. Technol.* **2011**, *41*, 317–335. [CrossRef]
12. Cao, S.; Wang, G.; Chen, L. Questionable value of planting thirsty trees in dry regions. *Nature* **2010**, *465*, 31. [CrossRef]
13. Qi, X.; Wang, K.; Zhang, C. Effectiveness of ecological restoration projects in a karst region of southwest china assessed using vegetation succession mapping. *Ecol. Eng.* **2013**, *54*, 245–253. [CrossRef]
14. Foley, J.A.; DeFries, R.; Asner, G.P.; Barford, C.; Bonan, G.; Carpenter, S.R.; Chapin, F.S.; Coe, M.T.; Daily, G.C.; Gibbs, H.K. Global consequences of land use. *Science* **2005**, *309*, 570–574. [CrossRef] [PubMed]
15. Song, X.-P.; Hansen, M.C.; Stehman, S.V.; Potapov, P.V.; Tyukavina, A.; Vermote, E.F.; Townshend, J.R. Global land change from 1982 to 2016. *Nature* **2018**, *560*, 639–643. [CrossRef] [PubMed]
16. Wang, F.; An, P.; Huang, C.; Zhang, Z.; Hao, J. Is afforestation-induced land use change the main contributor to vegetation dynamics in the semiarid region of north china? *Ecol. Indic.* **2018**, *88*, 282–291. [CrossRef]
17. Pei, J.; Wang, L.; Wang, X.; Niu, Z.; Kelly, M.; Song, X.-P.; Huang, N.; Geng, J.; Tian, H.; Yu, Y. Time series of landsat imagery shows vegetation recovery in two fragile karst watersheds in southwest china from 1988 to 2016. *Remote Sens.* **2019**, *11*, 2044. [CrossRef]
18. Liao, C.; Yue, Y.; Wang, K.; Fensholt, R.; Tong, X.; Brandt, M. Ecological restoration enhances ecosystem health in the karst regions of southwest china. *Ecol. Indic.* **2018**, *90*, 416–425. [CrossRef]
19. Zhao, J.; Yang, Y.; Zhao, Q.; Zhao, Z. Effects of ecological restoration projects on changes in land cover: A case study on the loess plateau in china. *Sci. Rep.* **2017**, *7*, 44496. [CrossRef]
20. O'Donnell, F.C.; Flatley, W.T.; Springer, A.E.; Fulé, P.Z. Forest restoration as a strategy to mitigate climate impacts on wildfire, vegetation, and water in semiarid forests. *Ecol. Appl.* **2018**, *28*, 1459–1472. [CrossRef]

21. Liang, S.; Hurteau, M.D.; Westerling, A.L. Large-scale restoration increases carbon stability under projected climate and wildfire regimes. *Front. Ecol. Environ.* **2018**, *16*, 207–212. [CrossRef]

22. Quéré, C.L.; Andrew, R.M.; Friedlingstein, P.; Sitch, S.; Pongratz, J.; Manning, A.C.; Korsbakken, J.I.; Peters, G.P.; Canadell, J.G.; Jackson, R.B. Global carbon budget 2017. *Earth Syst. Sci. Data* **2018**, *10*, 405–448. [CrossRef]

23. Chen, M.; Rafique, R.; Asrar, G.R.; Bond-Lamberty, B.; Ciais, P.; Zhao, F.; Reyer, C.P.; Ostberg, S.; Chang, J.; Ito, A. Regional contribution to variability and trends of global gross primary productivity. *Environ. Res. Lett.* **2017**, *12*, 105005. [CrossRef]

24. Wu, L.; Wang, S.; Bai, X.; Tian, Y.; Luo, G.; Wang, J.; Li, Q.; Chen, F.; Deng, Y.; Yang, Y. Climate change weakens the positive effect of human activities on karst vegetation productivity restoration in southern china. *Ecol. Indic.* **2020**, *115*, 106392. [CrossRef]

25. Zhang, Y.; Xiao, X.; Wu, X.; Zhou, S.; Zhang, G.; Qin, Y.; Dong, J. A global moderate resolution dataset of gross primary production of vegetation for 2000–2016. *Sci. Data* **2017**, *4*, 170165. [CrossRef] [PubMed]

26. Zhao, M.; Running, S.W. Drought-induced reduction in global terrestrial net primary production from 2000 through 2009. *Science* **2010**, *329*, 940–943. [CrossRef] [PubMed]

27. Zhao, M.; Heinsch, F.A.; Nemani, R.R.; Running, S.W. Improvements of the modis terrestrial gross and net primary production global data set. *Remote Sens. Environ.* **2005**, *95*, 164–176. [CrossRef]

28. Jiang, C.; Ryu, Y. Multi-scale evaluation of global gross primary productivity and evapotranspiration products derived from breathing earth system simulator (bess). *Remote Sens. Environ.* **2016**, *186*, 528–547. [CrossRef]

29. Ryu, Y.; Baldocchi, D.D.; Kobayashi, H.; van Ingen, C.; Li, J.; Black, T.A.; Beringer, J.; Van Gorsel, E.; Knohl, A.; Law, B.E. Integration of modis land and atmosphere products with a coupled-process model to estimate gross primary productivity and evapotranspiration from 1 km to global scales. *Glob. Biogeochem. Cycles* **2011**, *25*. [CrossRef]

30. Tong, X.; Brandt, M.; Yue, Y.; Horion, S.; Wang, K.; De Keersmaecker, W.; Tian, F.; Schurgers, G.; Xiao, X.; Luo, Y. Increased vegetation growth and carbon stock in china karst via ecological engineering. *Nat. Sustain.* **2018**, *1*, 44. [CrossRef]

31. Ma, J.; Xiao, X.; Miao, R.; Li, Y.; Chen, B.; Zhang, Y.; Zhao, B. Trends and controls of terrestrial gross primary productivity of china during 2000–2016. *Environ. Res. Lett.* **2019**, *14*, 084032. [CrossRef]

32. Qiu, B.; Chen, G.; Tang, Z.; Lu, D.; Wang, Z.; Chen, C. Assessing the three-north shelter forest program in china by a novel framework for characterizing vegetation changes. *ISPRS J. Photogramm. Remote Sens.* **2017**, *133*, 75–88. [CrossRef]

33. Chen, Y.; Gu, H.; Wang, M.; Gu, Q.; Ding, Z.; Ma, M.; Liu, R.; Tang, X. Contrasting performance of the remotely-derived gpp products over different climate zones across china. *Remote Sens.* **2019**, *11*, 1855. [CrossRef]

34. Yue, Y.; Wang, K.; Liu, B.; Li, R.; Zhang, B.; Chen, H.; Zhang, M. Development of new remote sensing methods for mapping green vegetation and exposed bedrock fractions within heterogeneous landscapes. *Int. J. Remote Sens.* **2013**, *34*, 5136–5153. [CrossRef]

35. Jiang, Z.; Lian, Y.; Qin, X. Rocky desertification in southwest china: Impacts, causes, and restoration. *Earth Sci. Rev.* **2014**, *132*, 1–12. [CrossRef]

36. Butscher, C.; Huggenberger, P. Modeling the temporal variability of karst groundwater vulnerability, with implications for climate change. *Environ. Sci. Technol.* **2009**, *43*, 1665–1669. [CrossRef] [PubMed]

37. Wang, S.; Liu, Q.; Zhang, D. Karst rocky desertification in southwestern china: Geomorphology, landuse, impact and rehabilitation. *Land Degrad. Dev.* **2004**, *15*, 115–121. [CrossRef]

38. Zhang, C.; Qi, X.; Wang, K.; Zhang, M.; Yue, Y. The application of geospatial techniques in monitoring karst vegetation recovery in southwest china: A review. *Prog. Phys. Geogr.* **2017**, *41*, 450–477. [CrossRef]

39. Delang, C.O.; Yuan, Z. *China's Grain for Green Program*; Springer: Cham, Switzerland, 2016.

40. Yuan, D. Rock desertification in the subtropical karst of south china. *Z. Geomorphol. Suppl.* **1997**, *108*, 81–90.

41. Zhang, Q.; Li, Y. Climatic variation of rainfall and rain day in southwest china for last 48 years. *Plateau Meteorol.* **2014**, *33*, 372–383.

42. Liu, J.; Liu, M.; Zhuang, D.; Zhang, Z.; Deng, X. Study on spatial pattern of land-use change in china during 1995–2000. *Sci. China Ser. D Earth Sci.* **2003**, *46*, 373–384.

43. Deng, X.; Huang, J.; Rozelle, S.; Uchida, E. Cultivated land conversion and potential agricultural productivity in china. *Land Use Policy* **2006**, *23*, 372–384. [CrossRef]

44. Li, W.; MacBean, N.; Ciais, P.; Defourny, P.; Lamarche, C.; Bontemps, S.; Houghton, R.A.; Peng, S. Gross and net land cover changes in the main plant functional types derived from the annual esa cci land cover maps (1992–2015). *Earth Syst. Sci. Data* **2018**, *10*, 219. [CrossRef]

45. Zhou, Q.; Li, B.; Kurban, A. Trajectory analysis of land cover change in arid environment of china. *Int. J. Remote Sens.* **2008**, *29*, 1093–1107. [CrossRef]

46. Wang, D.; Gong, J.; Chen, L.; Zhang, L.; Song, Y.; Yue, Y. Spatio-temporal pattern analysis of land use/cover change trajectories in xihe watershed. *Int. J. Appl. Earth Obs. Geoinf.* **2012**, *14*, 12–21. [CrossRef]

47. Baral, P.; Wen, Y.; Urriola, N.N. Forest cover changes and trajectories in a typical middle mountain watershed of western nepal. *Land* **2018**, *7*, 72. [CrossRef]

48. Watson, R.T.; Noble, I.R.; Bolin, B.; Ravindranath, N.; Verardo, D.J.; Dokken, D.J. *IPCC Special Report on Land Use, Land-Use Change, and Forestry*; Intergovernmental Panel on Climate Change: Geneva, Switzerland, 2000.

49. Chen, C.; Park, T.; Wang, X.; Piao, S.; Xu, B.; Chaturvedi, R.K.; Fuchs, R.; Brovkin, V.; Ciais, P.; Fensholt, R. China and india lead in greening of the world through land-use management. *Nat. Sustain.* **2019**, *2*, 122–129. [CrossRef]

50. Weijing, L.; Chenghu, S.; Jinqing, Z.; Ruonan, Z.; Jingpeng, L. Characteristics of wet and dry seasons in southwest china during 1961–2014. *Adv. Clim. Chang. Res.* **2017**, *13*, 103.

51. Du, W.; Yan, H.; Zhen, L.; Hu, Y. The experience and practice of desertification control in karst region of southwest china. *Acta Ecol. Sin.* **2019**, *39*, 5798–5808.

52. Huang, R.; Liu, Y.; Wang, L.; Wang, L. Analyses of the causes of severe drought occurring in southwest china from the fall of 2009 to the spring of 2010. *Chin. J. Atmos. Sci.* **2012**, *36*, 443–457.

53. Li, X.; Li, Y.; Chen, A.; Gao, M.; Slette, I.J.; Piao, S. The impact of the 2009/2010 drought on vegetation growth and terrestrial carbon balance in southwest china. *Agric. For. Meteorol.* **2019**, *269*, 239–248. [CrossRef]

54. Tong, X.; Wang, K.; Brandt, M.; Yue, Y.; Liao, C.; Fensholt, R. Assessing future vegetation trends and restoration prospects in the karst regions of southwest china. *Remote Sens.* **2016**, *8*, 357. [CrossRef]

55. Xu, Y.; Yang, J.; Chen, Y. Ndvi-based vegetation responses to climate change in an arid area of china. *Theor. Appl. Climatol.* **2016**, *126*, 213–222. [CrossRef]

56. Liu, Y.; Li, Y.; Li, S.; Motesharrei, S. Spatial and temporal patterns of global ndvi trends: Correlations with climate and human factors. *Remote Sens.* **2015**, *7*, 13233–13250. [CrossRef]

57. Ichii, K.; Kawabata, A.; Yamaguchi, Y. Global correlation analysis for ndvi and climatic variables and ndvi trends: 1982–1990. *Int. J. Remote Sens.* **2002**, *23*, 3873–3878. [CrossRef]

58. Wang, J.; Dong, J.; Yi, Y.; Lu, G.; Oyler, J.; Smith, W.; Zhao, M.; Liu, J.; Running, S. Decreasing net primary production due to drought and slight decreases in solar radiation in china from 2000 to 2012. *J. Geophys. Res. Biogeosci.* **2017**, *122*, 261–278. [CrossRef]